

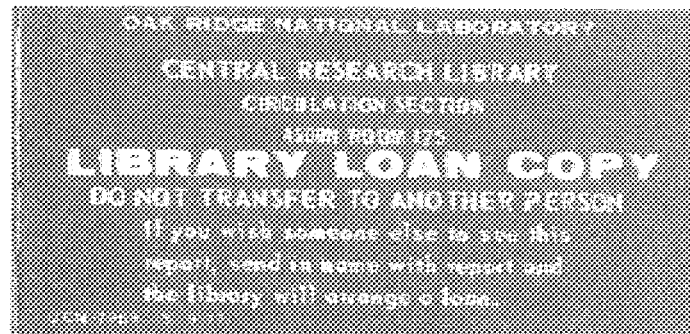
ornl

OAK RIDGE
NATIONAL
LABORATORY

MARTIN MARIETTA

Initial Effects of Nuclear Weapon X-Radiation on the LAMPSHADE Orbital Debris Satellite Shield

M. S. Smith
R. T. Santoro



OPERATED BY
MARTIN MARIETTA ENERGY SYSTEMS, INC.
FOR THE UNITED STATES
DEPARTMENT OF ENERGY

This report has been reproduced directly from the best available copy.

Available to DOE and DOE contractors from the Office of Scientific and Technical Information, P.O. Box 62, Oak Ridge, TN 37831; prices available from (615) 576-8401, FTS 626-8401.

Available to the public from the National Technical Information Service, U.S. Department of Commerce, 5255 Port Royal Rd., Springfield, VA 22161.

NTIS price codes—Printed Copy: A03 Microfiche A01

This report was prepared as an account of work sponsored by an agency of the United States Government. Neither the United States Government nor any agency thereof, nor any of their employees, makes any warranty, express or implied, or assumes any legal liability or responsibility for the accuracy, completeness, or usefulness of any information, apparatus, product, or process disclosed, or represents that its use would not infringe privately owned rights. Reference herein to any specific commercial product, process, or service by trade name, trademark, manufacturer, or otherwise does not necessarily constitute or imply its endorsement, recommendation, or favoring by the United States Government or any agency thereof. The views and opinions of authors expressed herein do not necessarily state or reflect those of the United States Government or any agency thereof.

ORNL/TM-11321

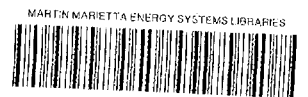
Engineering Physics and Mathematics

**Initial Effects of Nuclear Weapon X-Radiation on
the LAMPSHADE Orbital Debris Satellite Shield**

M. S. Smith and R. T. Santoro

DATE PUBLISHED — September 1989

Prepared by the
OAK RIDGE NATIONAL LABORATORY
Oak Ridge, Tennessee 37831
operated by
MARTIN MARIETTA ENERGY SYSTEMS, INC.
for the
U.S. DEPARTMENT OF ENERGY
under contract DE-AC05-84OR21400



3 4456 0327586 3

CONTENTS

ABSTRACT	ix
1. INTRODUCTION	1
2. DETAILS OF THE CALCULATIONS	2
3. DISCUSSION OF RESULTS	5
4. CONCLUSIONS AND RECOMMENDATIONS FOR FUTURE WORK	14
REFERENCES	15

LIST OF FIGURES

<u>Figure</u>		<u>Page</u>
1	Lampshade Debris Shield Concept	3
2	Density vs. depth for tantalum at 250 nsec from the 3 keV, 30 cal/cm ² source term	9
3	Impulse vs. time when 1 and 3 keV x-rays are incident on the lead shield at 3 cal/cm ² with a 250 ns lognormal time distribution . . .	11
4.	Impulse vs. time when 1 keV blackbody and weapon spectrum x-rays are incident on the tantalum liquidator at 1 cal/cm ² with a 100 ns lognormal time distribution	12
5	Impulse vs. time when 1 and 3 keV monoenergetic x-rays are incident on the tantalum liquidator at 30 cal/cm ² with a 250 ns lognormal time distribution	13

LIST OF TABLES

<u>Table</u>		<u>Page</u>
1	Material Properties for Lead and Tantalum	4
2	Lead—Mass Fraction by Phase	6
3	Tantalum—Mass Fraction by Phase	7

ABSTRACT

One-dimensional thermal-hydrodynamic calculations have been carried out to estimate the response of the lead bumper plate and tantalum liquidation screen of the LAMPSHADE orbital debris satellite shield. The mass loss fraction in the solid, liquid, and vapor phases as a function of time after irradiation for several typical incident x-ray spectra and fluences were calculated using the PUFF-TFT code. The material losses did not exceed 2% and fracture and spallation were confined to the surface region with no apparent reduction in the performance of these components against incident debris.

1. INTRODUCTION

A novel concept for shielding satellites against orbital debris and ground launched projectiles was recently introduced by JAYCOR.¹ This shield concept is designed to provide full coverage (in the direction of flight) of satellites against orbital debris and projectiles having a broad range of kinetic energies ($m = 0 - 30$ g; $v = 1 - 15$ km/s). Unlike dual plate designs,^{2,3} LAMPSHADE is a monolithic scheme based principally on physics and configuration arguments rather than on material considerations. It is purported by the designers to be the simplest design that provides simultaneous protection against both directional orbital debris and ground launched projectiles.

This study was carried out to estimate the response of LAMPSHADE to x-radiation from space detonated nuclear weapons to establish criteria for material selection and disposition. The damage to the different components of the shield can also be used to guide satellite and sensor designers with information on the amount of shield material blown off as the result of the x-ray impulse that could possibly blind the sensors or otherwise contaminate the satellite.

The nuclear response of the LAMPSHADE components was calculated using the one-dimensional radiation transport/hydrocode PUFF-TFT.⁴ Details of the calculations including the shield model, material properties, and incident x-ray parameters are given in Section 2. The response of the shield as a function of incident x-ray energy, loading, and temporal distributions are presented and discussed in Section 3. The conclusions from this study and suggestions for future investigations are given in Section 4.

2. DETAILS OF THE CALCULATIONS

The LAMPSHADE shield and a description of the components is given in Figure 1. The shield consists of a wedge shaped bumper plate assembly that provides the satellite with 360-deg protection against orbital debris. The wedge angle ensures that incident projectile collisions occur at oblique angles (15-deg) to the bumper plate surface. An alternative design, also shown in the figure, includes a thin screen placed ahead of the vertex of the wedge that breaks up (liquidates) the projectiles to further reduce the mass of the projectile that impinges on the bumper. In the measurements carried out to determine shield performance for projectiles launched using a light gas gun, JAYCOR selected lead as the bumper material and aluminum foam or tantalum for the liquidator screen.

Separate radiation response calculations were made for x-rays normally incident on a 0.575-g/cm²-thick lead bumper plate and also on a 0.21-g/cm²-thick tantalum liquidator screen. While JAYCOR also investigated the shield performance using a thicker liquidator screen (1.67 g/cm²), the nuclear calculations were made only for the thinner screen. As noted above, the incident radiation was taken to be normal to the material surface and no corrections or calculations were made to account for radiation incident at oblique angles to the surface normal. Several efforts were made to calculate the nuclear response of an aluminum foam liquidator screen. However, logic errors were discovered in the PUFF-TFT modules that treat the hydrodynamic response of foam materials so these calculations were terminated. Efforts to repair this shortcoming were made, but the extent of the required programming was beyond the scope of this effort.

The material properties for lead and tantalum used in the PUFF-TFT calculations are summarized in Table 1. These data were obtained from the literature and, in some cases, are best estimates. Previous experience has shown that these values yield valid results.

Several x-ray spectral distributions were studied to ensure that the survivability criteria of the LAMPSHADE components were evaluated over a wide range of incident radiation scenarios and parameters. The nuclear response of the lead bumper plate was estimated for five incident spectra having 250 ns lognormal time distributions:

- monoenergetic 1 and 3 keV x-rays at loadings of 1 and 3 cal/cm², and a
- 1 keV blackbody spectrum at 1 cal/cm².

The response of the tantalum liquidator screen was calculated for eight different incident spectra:

- monoenergetic 1 keV x-rays at 1, 3, and 30 cal/cm² each having 250 ns lognormal time distributions,
- monoenergetic 3 keV x-rays at 3 and 30 cal/cm² each having 250 ns lognormal time distributions,
- 1 keV blackbody spectrum at 1 cal/cm² for both 100 and 250 ns lognormal distributions, and
- x-ray energies corresponding to those found in a typical weapon.

	Bumper Plate	Liquidator
Material	Pb	Ta
Areal Density (g/cm ²)	0.575	0.21

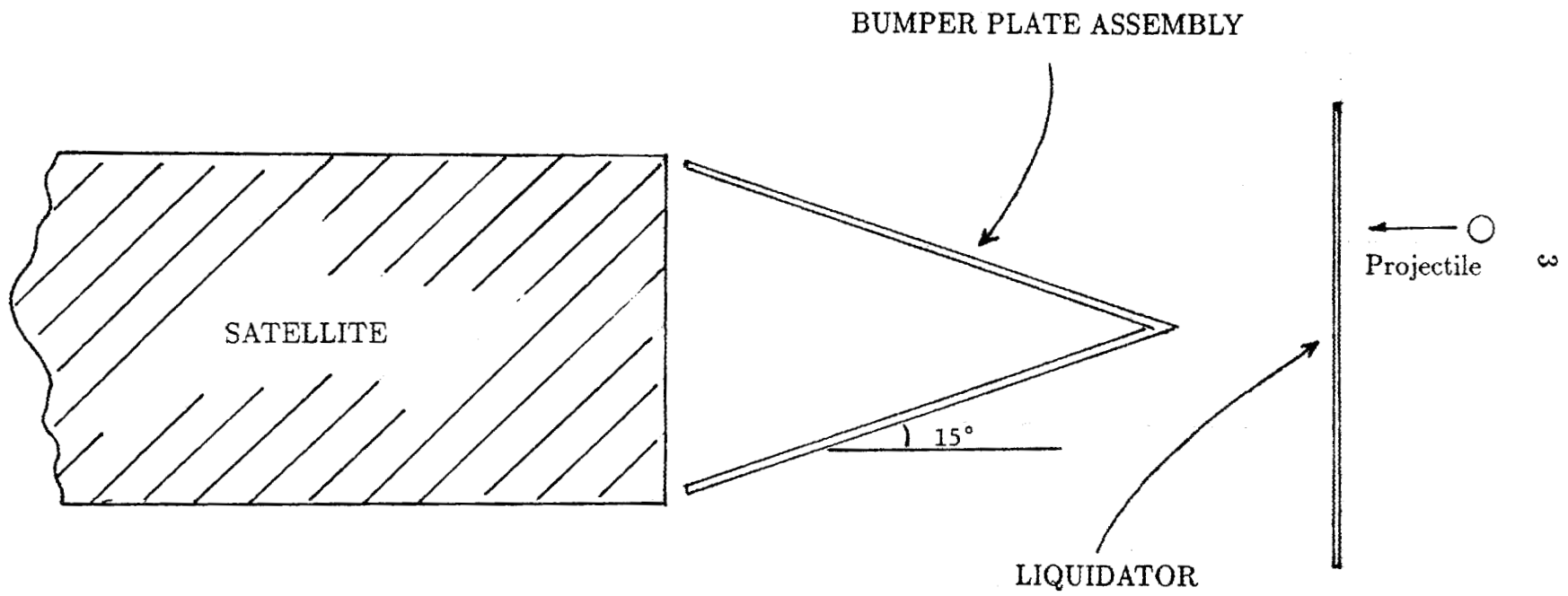


Figure 1. Lampshade Debris Shield Concept.
(Not to scale)

Table 1

Material Properties for Lead and Tantalum

Parameter	Lead	Tantalum
Density (g/cm ³)	11.30	16.60
Bulk Modulus (dyne/cm ²)	5.0E(11)*	1.94E(12)
Shear Modulus (dyne/cm ²)	5.56E(10)	7.11E(11)
Yield Strength (dyne/cm ²)	1.31E(08)	1.40E(10)
Spall Strength (dyne/cm ²)	0.17E(10)	-2.0E(10)
Gruneisen Constant	2.20	1.69
Perfect Gas Constant	0.25	0.25
Sublimation energy (cal/g)	9.16E(09)	2.66E(02)
Specific heat - full melt (cal/g)	0.033	0.041
Melt energy (cal/g)	9.8	127.7
Latent heat of fusion (cal/g)	5.5	994.5

* Read as 5.0×10^{11}

3. DISCUSSION OF RESULTS

The survivability of the LAMPSHADE shield was evaluated by calculating the one-dimensional thermo-mechanical response of the components of the shield to the incident x-ray spectra described above. Two issues were studied: the mechanical integrity of the shield following exposure to the threat and the amount of material blown off the surfaces of the shield that have potential for blinding or otherwise reducing the effectiveness of the sensors and windows on the satellite.

To provide insight into the magnitude of these effects, the mass fractions by phase results are presented. That is, for each incident radiation source, the fractions of lead or tantalum that exist in the solid, liquid, and vapor states are given as a function of time after irradiation.

The results obtained for the lead bumper plate are summarized in Table 2. For these cases, a 250 ns lognormal time distribution was assumed for each of the incident x-ray threats. The mass fractions by phase are tabulated at 50, 80, 100, 150, 200, and 250 ns after arrival of the incident radiation. These results show that the amounts of material in the liquid or vapor state are small for all of the cases that were examined. For the five incident radiation threats, only the 1 keV blackbody spectrum at 1 cal/cm² appears to be damaging (based on comparison of the solid mass fractions at 250 ns).

The results in Table 2 show that only small portions of the shield material are lost due to phase changes. The remaining solid material may also suffer mechanical degradation due to spalls or fractures within the medium. Spall/fracture flags in the PUFF code showed that the 1 keV, 3 cal/cm² x-ray source term produced deep spalls within the solid portion of the medium. In contrast, the 3 keV monoenergetic source terms and the 1 keV blackbody spectrum had no spall indications within the solid, and the solid fraction probably retains its mechanical integrity over the 250 nanosecond time frame.

Results for the tantalum liquidator are provided in Table 3. Here also, only a small fraction of material is lost due to phase changes. These results are, however, more in line with expectations. For the monoenergetic source terms, the higher temperature x-rays cause greater damage for the same wall loading, and the larger wall loadings are more damaging. A plot of density vs. depth at 250 nsec for the 3 keV, 30 cal/cm² source term is provided in Figure 2.

The time dependence of the radiation distribution was also examined for a 1 keV blackbody spectrum. For the case of a 100 nanosecond lognormal time distribution, a greater fraction of material undergoes a phase change, and at a more rapid pace, however, more material was vaporized using the 250 nanosecond lognormal time distribution. The blowoff from the 1 keV blackbody spectrum is greater than that from the 1 keV x-ray source term for the same wall loading and time distribution (i.e., 1 cal/cm² and 250 ns). The weapon spectrum, with the highest average x-ray energy, is the most benign source term considering the relatively rapid energy deposition in the tantalum.

Each of the tantalum cases exhibited a reduction in the spall strength in the solid region near the interface with the liquid fraction. Typically, this was a factor of two reduction, extending approximately 5×10^{-4} cm into the solid region. In addition, the 1 keV, 1 cal/cm² x-ray source term showed fracture damage in the

Table 2
Lead
Mass Fraction by Phase

Time (sec)	Solid	Liquid	Vapor
	1 keV X-rays at 1 cal/cm ²		
5.0-08	9.988-01	7.428-05	1.151-03
8.0-08	9.968-01	1.219-03	2.019-03
1.0-07	9.961-01	1.509-03	2.417-03
1.5-07	9.947-01	2.177-03	3.125-03
2.0-07	9.936-01	2.760-03	3.626-03
2.5-07	9.930-01	3.107-03	3.926-03
	1 keV X-rays at 3 cal/cm ²		
5.0-08	9.972-01	1.036-03	1.782-03
8.0-08	9.961-01	1.362-03	2.568-03
1.0-07	9.954-01	1.726-03	2.915-03
1.5-07	9.942-01	2.185-03	3.626-03
2.0-07	9.932-01	2.612-03	4.164-03
2.5-07	9.922-01	3.500-03	4.337-03
	3 keV X-rays at 1 cal/cm ²		
5.0-08	9.972-01	1.482-03	1.337-03
8.0-08	9.957-01	1.571-03	2.729-03
1.0-07	9.949-01	1.829-03	3.239-03
1.5-07	9.936-01	2.297-03	4.089-03
2.0-07	9.926-01	2.744-03	4.641-03
2.5-07	9.918-01	3.089-03	5.068-03
	3 keV X-rays at 3 cal/cm ²		
5.0-08	9.961-01	1.509-03	2.416-03
8.0-08	9.947-01	1.530-03	3.771-03
1.0-07	9.939-01	1.828-03	4.262-03
1.5-07	9.926-01	2.317-03	5.068-03
2.0-07	9.918-01	2.609-03	5.549-03
2.5-07	9.910-01	2.937-03	6.090-03
	1 keV Blackbody at 1 cal/cm ²		
5.0-08	9.966-01	2.321-03	1.040-03
8.0-08	9.939-01	3.176-03	2.915-03
1.0-07	9.930-01	3.261-03	3.771-03
1.5-07	9.912-01	3.959-03	5.068-03
2.0-07	9.900-01	4.457-03	5.549-03
2.5-07	9.895-01	4.451-03	6.090-03

Table 3
Tantalum
Mass Fraction by Phase

Time (sec)	Solid	Liquid	Vapor
	1 keV X-rays at 1 cal/cm ²		
5.0-08	1.0		
8.0-08	9.987-01	2.885-04	1.010-03
1.0-07	9.973-01	1.731-03	1.010-03
1.5-07	9.961-01	2.885-03	1.010-03
2.0-07	9.978-01	1.154-03	1.010-03
2.5-07	9.990-01		1.010-03
	1 keV X-rays at 3 cal/cm ²		
5.0-08	9.978-01	1.154-03	1.010-03
8.0-08	9.929-01	5.337-03	1.731-03
1.0-07	9.914-01	6.733-03	1.875-03
1.5-07	9.889-01	9.193-03	1.875-03
2.0-07	9.886-01	9.545-03	1.875-03
2.5-07	9.896-01	8.542-03	1.875-03
	3 keV X-rays at 3 cal/cm ²		
5.0-08	9.962-01	1.616-03	2.885-04
8.0-08	9.904-01	6.531-03	3.029-03
1.0-07	9.889-01	7.462-03	3.606-03
1.5-07	9.865-01	9.880-03	3.606-03
2.0-07	9.855-01	1.087-02	3.606-03
2.5-07	9.865-01	9.880-03	3.606-03
	1 keV X-rays at 30 cal/cm ²		
5.0-08	9.914-01	4.858-03	3.751-03
8.0-08	9.886-01	6.660-03	4.757-03
1.0-07	9.874-01	7.677-03	4.904-03
1.5-07	9.855-01	9.560-03	4.904-03
2.0-07	9.850-01	1.010-02	4.904-03
2.5-07	9.860-01	9.055-03	4.904-03
	3 keV X-rays at 30 cal/cm ²		
5.0-08	9.882-01	5.301-03	3.375-03
8.0-08	9.844-01	6.750-03	8.828-03
1.0-07	9.825-01	8.158-03	9.304-03
1.5-07	9.803-01	1.011-02	9.560-03
2.0-07	9.803-01	1.011-02	9.560-03
2.5-07	9.811-01	9.336-03	9.560-03

Table 3
(continued)

Time	Solid	Liquid	Vapor
1 keV Blackbody at 1 cal/cm ² 250 nsec lognormal time dependence			
5.0-08	1.0		
8.0-08	9.984-01	1.587-03	
1.0-07	9.941-01	3.606-03	2.308-03
1.5-07	9.926-01	5.048-03	2.308-03
2.0-07	9.931-01	4.616-03	2.308-03
2.5-07	9.926-01	5.048-03	2.308-03
1 keV Blackbody at 1 cal/cm ² 100 nsec lognormal time dependence			
1.0-08	1.0		
2.0-08	1.0		
4.0-08	9.938-01	4.471-03	1.731-03
6.0-08	9.909-01	7.328-03	1.731-03
1.0-07	9.907-01	7.572-03	1.731-03
1.5-07	9.928-01	5.481-03	1.731-03
Weapon Spectrum at 1 cal/cm ² 100 nsec lognormal time dependence			
1.0-08	1.0		
2.0-08	1.0		
4.0-08	9.978-01	2.163-03	
6.0-08	9.961-01	2.019-03	1.875-03
1.0-07	9.981-01		1.875-03
1.5-07	9.981-01		1.875-03

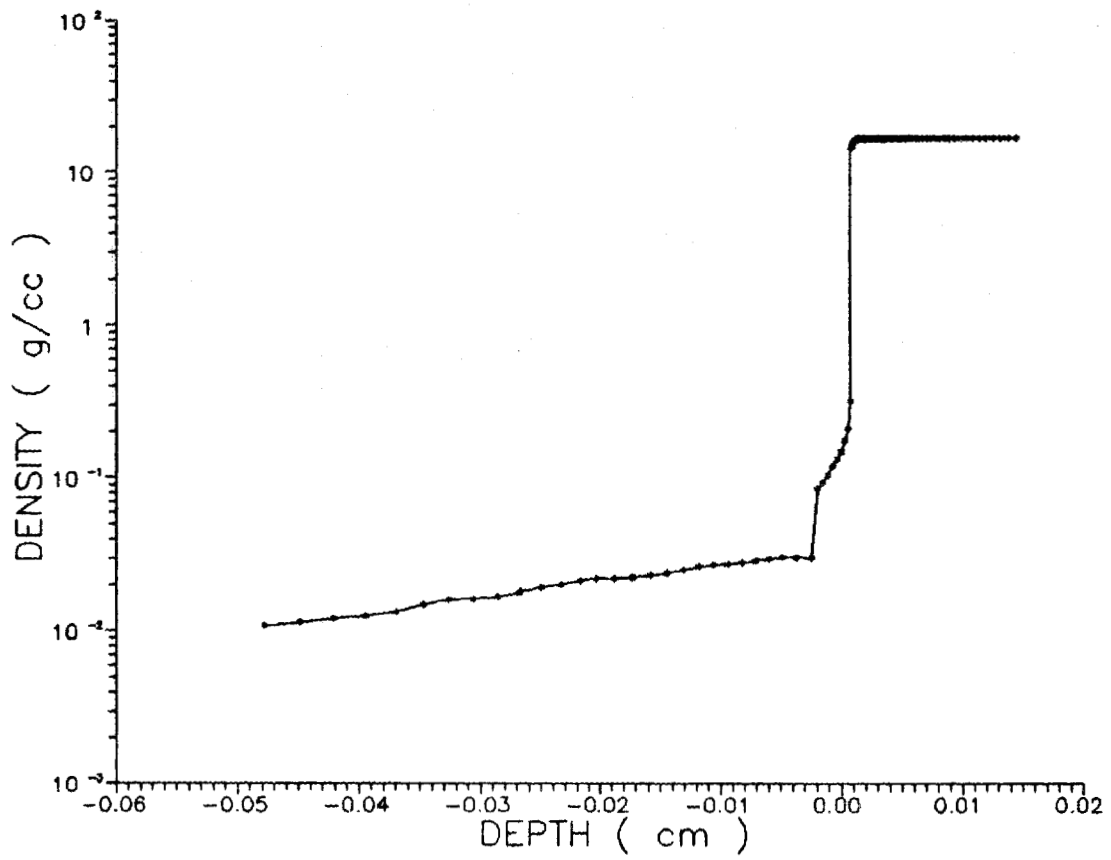


Figure 2. Density vs. depth for tantalum at 250 nsec from the 3 keV, 30 cal/cm² source term.

solid region. The two 100 nanosecond lognormal time distribution cases experienced extensive spallation after the source term was switched off, resulting in fracture layers extending a short distance into the solid region.

The time dependence of the impulse loading on the lead shield and tantalum liquidator plate is shown in Figures 3-5. These data provide the necessary information for designing mounting and shock-absorbing assemblies when the shield components are attached to the satellite. For a 3 cal/cm^2 loading by 1 and 3 keV x-rays having a 250 ns lognormal pulse distribution, the impulse peaks at 150 and 230 taps, respectively. In the case of a 1 cal/cm^2 x-ray loading on tantalum shown in Figure 4, the impulse peaks at 50 taps for a 1 keV blackbody spectrum and at 19 taps for the weapon spectrum. The discontinuities in the impulse curves at about 30 and 50 ns show the change in impulse during the phase transition. The impulse to the tantalum liquidator when the loading is 30 cal/cm^2 is plotted in Figure 5. For this case, the loads are 950 and 700 taps for 3 and 1 keV x-rays distributed in a 250 ns lognormal distribution.

The lead and tantalum components of the shield also provide adequate protection of the satellite against all of the incident x-ray sources. For example, for the 1 keV blackbody and weapon spectra, the radiation incident on the satellite is reduced by over two orders of magnitude. For all of the other incident radiation spectra, the flux on the satellite is essentially zero. It should be noted, however, that as currently envisioned, the LAMP SHADE concept does not provide 4π coverage of the satellite so additional shielding will be required to fully isolate the satellite components from damaging radiation.

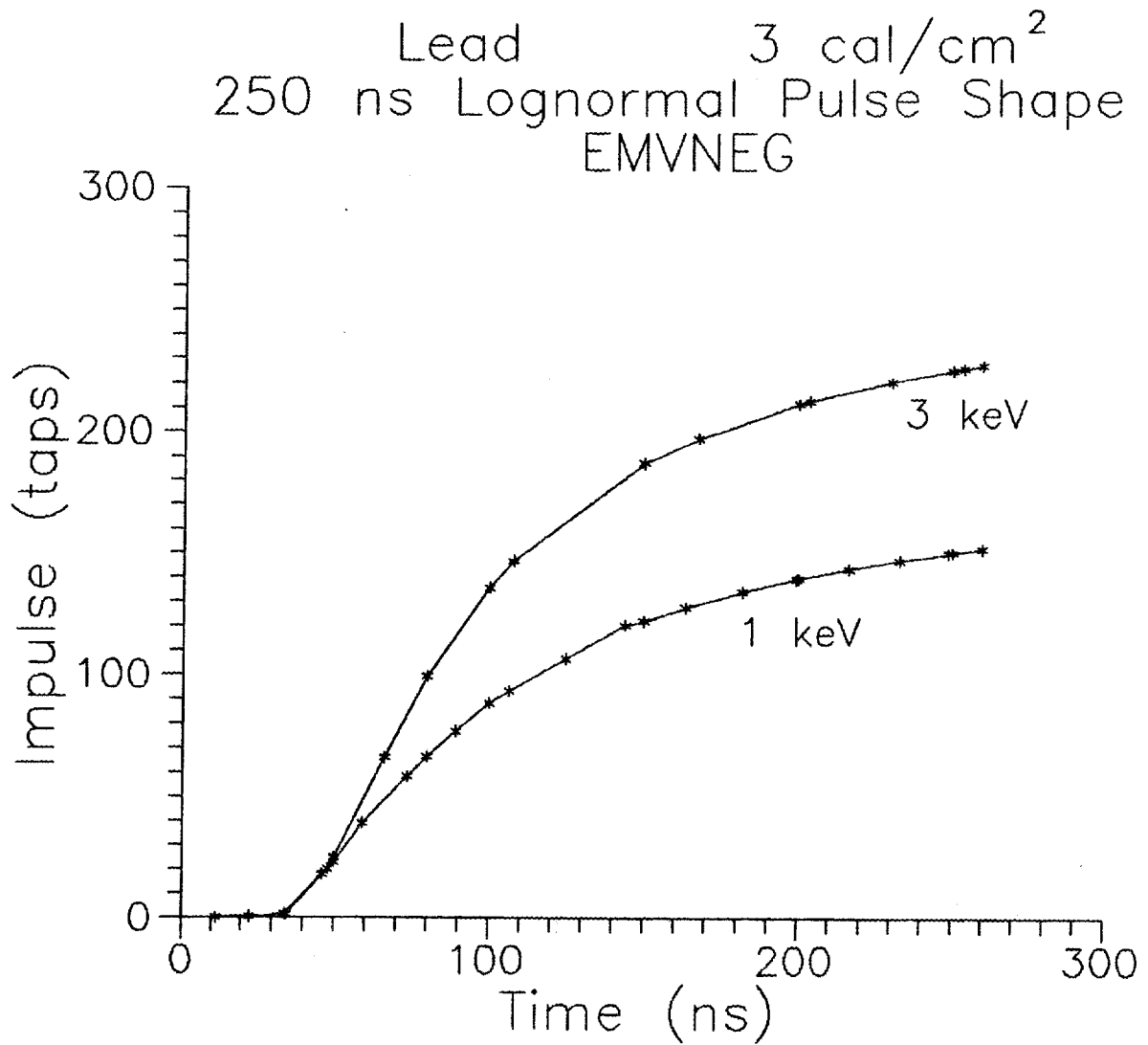


Figure 3. Impulse vs. time when 1 and 3 keV x-rays are incident on the lead shield at 3 cal/cm² with a 250 ns lognormal time distribution.

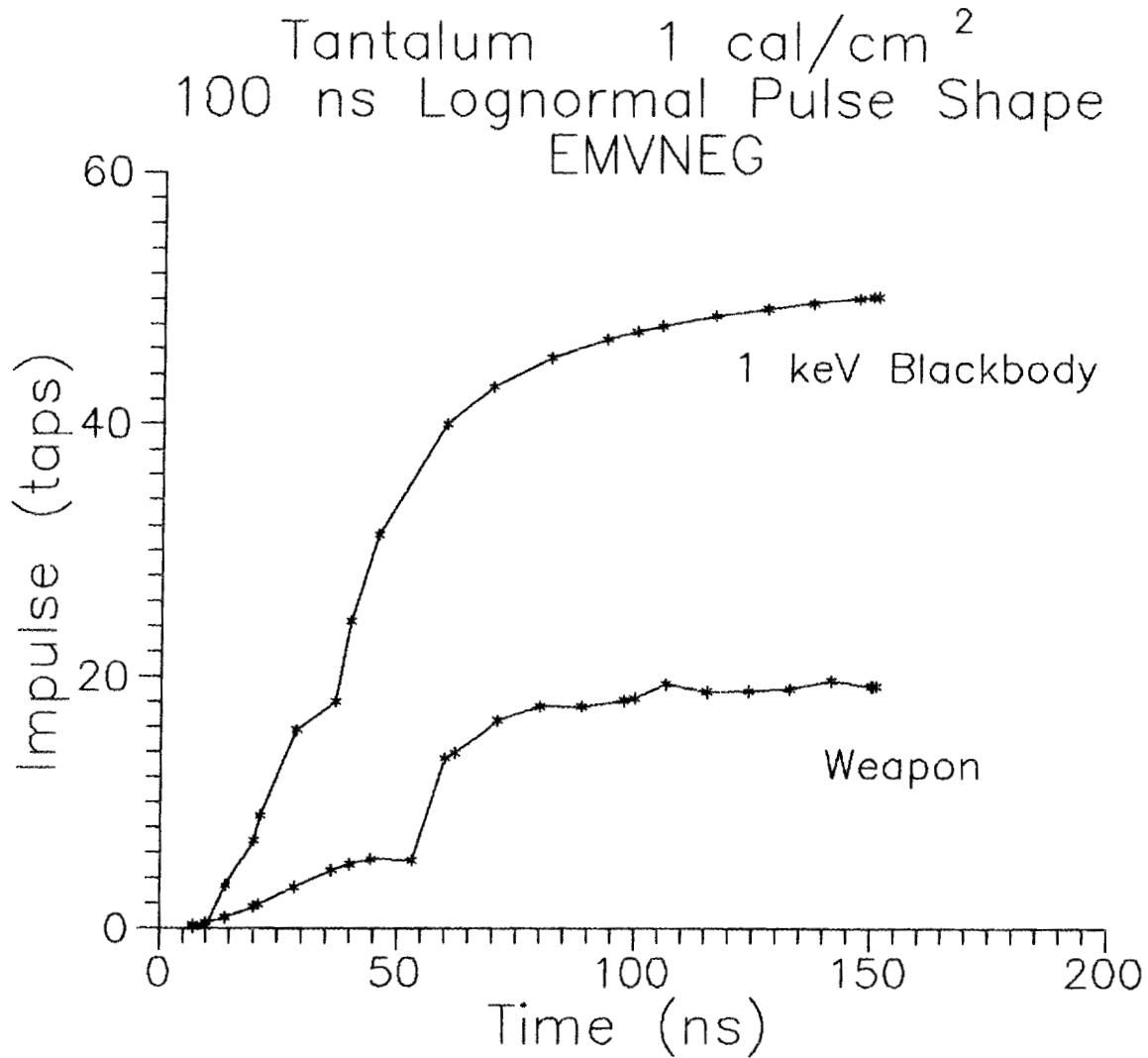


Figure 4. Impulse vs. time when 1 keV blackbody and weapon spectrum x-rays are incident on the tantalum liquidator at 1 cal/cm^2 with a 100 ns lognormal time distribution.

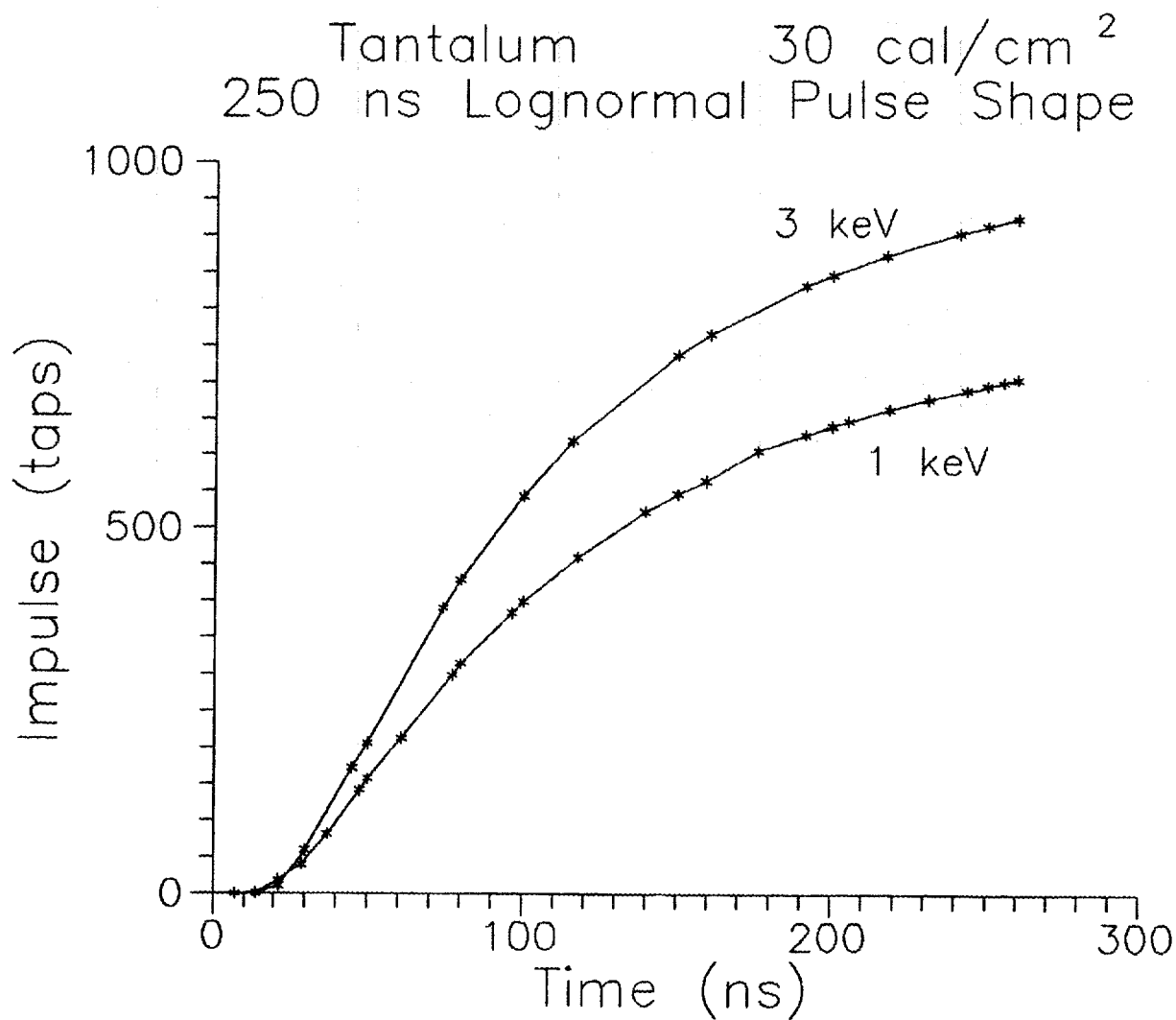


Figure 5. Impulse vs. time when 1 and 3 keV monoenergetic x-rays are incident on the tantalum liquidator at 30 cal/cm² with a 250 ns lognormal time distribution.

4. CONCLUSIONS AND RECOMMENDATIONS FOR FUTURE WORK

The material loss for the lead and tantalum components of the LAMPSHADE shield did not exceed 2% for any of the source terms investigated. While these material losses are small, there is no mechanism within these calculations to assess the effects of blown-off materials on sensors, windows, and optical equipment. Estimating these effects requires further study. Fracture damage within the solid region of the lead was sporadic, occurring only for the 1 keV, 3 cal/cm² x-rays source term. For spectra with short time depositions, tantalum sustained extensive fractures and spallation within the solid region near the liquid interface after the source term was switched off. The spall strength was also reduced near the liquid interface.

Additional work needs to be done to characterize the critical aspects of the source terms: temperature and energy distribution. In addition, higher fluences and shorter deposition times should be considered. Longer problem times should also be studied. Because of funding limitations, these cases investigated here were terminated at the end of the energy deposition. However, it may be prudent to run the problems to longer energy deposition times to see what happens during the "cooldown" phase.

REFERENCES

1. "Lightweight Attached Monolithic Protection Shield Against Debris," LAMPSHADE, presented to the Survivability Division, Strategic Defense Initiative Organization, March 22, 1989, JAYCOR, Inc.
2. F. L. Whipple, *Astronomical J.*, No. 1161:131 (1947).
3. B. G. Cour-Palais, "Space Vehicle Meteoroid Design," ESA-SP-153, 85-92 (1979) and also *Int. J. Impact Eng.* **5**, 221-238 (1987).
4. A. J. Watts, C. Breen, S. Sauer, and F. Smith, "Thin Film Transport (PUFF-TFT) Computer Code Development," AFWL-TR-88-66, Parts 1 and 2, Air Force Weapons Laboratory, Kirtland AFB, NM, June 1988.

INTERNAL DISTRIBUTION

- | | |
|----------------------|---|
| 1. B. R. Appleton | 13-17. R. T. Santoro |
| 2. Y. Y. Azmy | 18-22. M. S. Smith |
| 3. J. M. Barnes | 23. D. G. Thomas |
| 4. D. E. Bartine | 24. EPMD Reports Office |
| 5. T. J. Burns | 25-26. Laboratory Records
Department |
| 6. C. M. Haaland | 27. Laboratory Records,
ORNL-RC |
| 7. D. T. Ingersoll | 28. Document Reference
Section |
| 8. J. O. Johnson | 29. Central Research Library |
| 9. F. C. Maienschein | 30. ORNL Patent Section |
| 10. J. R. Merriman | |
| 11. V. Protopopescu | |
| 12. W. A. Rhoades | |

EXTERNAL DISTRIBUTION

31. 1Lt Dale R. Atkinson, AFWL/NTCOA, Air Force Weapons Laboratory, Kirtland Air Force Base, New Mexico 87117
32. 2Lt Mike Black, AFWL/NTCOA, Air Force Weapons Laboratory, Kirtland Air Force Base, New Mexico 87117
33. Prof. John J. Dorning, Department of Nuclear Engineering and Engineering Physics, Thornton Hall, McCormick Road, University of Virginia, Charlottesville, Virginia 22901
34. Dr. Franklin Felber, JAYCOR, P.O. Box 85154, San Diego, California 92138-9259
35. Prof. Robert M. Haralick, Boeing Clairmont Egtvedt Prof., Department of Electrical Engineering, Director, Intelligent Systems Lab., University of Washington, 402 Electrical Engineering Building, FT-10, Seattle, Washington 98195
36. Dr. James E. Leiss, 13013 Chestnut Oak Drive, Gaithersburg, Maryland 20878
37. Prof. Neville Moray, Department of Mechanical and Industrial Engineering, University of Illinois, 1206 West Green Street, Urbana, Illinois 61801
38. Prof. Mary F. Wheeler, Mathematics Department, University of Houston, 4800 Calhoun, Houston, Texas 77204-3476
- 39-48. Office of Scientific and Technical Information, P.O. Box 62, Oak Ridge, Tennessee 37830
49. Office of the Assistant Manager for Energy Research and Development, Department of Energy, Oak Ridge Operations, P.O. Box 2001, Oak Ridge, TN 37831